

Efficient Degradation of Sulfamethoxazole by the Fe(II)/HSO₅⁻ Process Enhanced by Hydroxylamine: Efficiency and Mechanism

Abstract

Fenton or Fenton-like processes have been regarded as feasible methods to degrade a wide variety of contaminants by generating reactive species, but the efficiency is highly affected by the slow transformation from Fe(III) to Fe(II) as well as pH. This study proposed a method by adding hydroxylamine (HA) to the Fe(II)/HSO₅⁻ (Fe(II)/PMS) process to accelerate the degradation of contaminants, selecting a broad-spectrum sulfonamide antibiotic - sulfamethoxazole (SMX) - as the target compounds. The degradation efficiency and mechanism of SMX by the HA/Fe(II)/PMS process was elucidated for the first time. Compared with Fe(II)/PMS process, HA/Fe(II)/PMS process showed about 4 times higher degradation efficiency of SMX at pH 3.0 and it also exhibited high efficiency in a wider range of pH (3.0-6.0). The addition of HA enhanced the transformation of Fe(III) to Fe(II), which participated in the formation of reactive species as electron donor. Based on the experiments of alcohols quenching and competition kinetics between benzoic acid and SMX, the mechanism study indicated that both the sulfate radicals (SO₄^{•-}) and the hydroxyl radical (HO[•]) resulted in the degradation of SMX, with the latter regarded as the dominant reactive species. Furthermore, degradation intermediates of SMX were analyzed, and three main transformation pathways were thus proposed, including the cleavage of S-N bond, oxidation of amine group on the aromatic ring, and hydroxylation of the benzene ring. The HA/Fe(II)/PMS process was also effective in removal of SMX and total organic carbon (TOC) from the real pharmaceutical wastewater. This work would broaden the scope of application of Fenton and Fenton-like processes enhanced by HA in treatment of contaminants.

Keywords: Sulfate radical; Hydroxyl radical; Peroxomonosulfate; Hydroxylamine; Sulfamethoxazole; Mechanism

1. Introduction

An increasing number of antibiotics are environmentally widespread and routinely found in aquatic environment including effluent of wastewater treatment plant, surface water, even drinking water (Kümmerer, 2009; Rivera-Utrilla et al., 2013), and they are of great concern for their toxicity and potential to induce resistance of drug acting on aquatic ecosystems and human health (Marx et al., 2015; Pomati et al., 2006). Industrial pharmaceutical wastewater treatment plants without effective treatment of antibiotics have become a significant threat for aquatic environment (Larsson, 2007).

Conventional treatment processes exhibit poor removal for antibiotics from pharmaceutical wastewater (Michael et al., 2013). Advanced oxidation processes (AOPs) based on hydroxyl radical (HO[•]) oxidation, such as photolysis (Ryan et al., 2011), electrochemical oxidation (De Amorim et al., 2013), and catalytic ozonation (Gonçalves et al., 2012) have indicated a certain success in the degradation of antibiotics. Recently, increasing attention has been paid to the catalytic peroxymonosulfate (HSO₅⁻, PMS) oxidation based on sulfate radicals (SO₄^{•-}) due to its high efficiency of selection and degradation for some refractory organic contaminants (Neta et al., 1988). Having a comparable oxidizing ability of HO[•] ($E^0 = 1.9-2.7V$) (Buxton et al., 1988), SO₄^{•-} with E^0 of 2.5-3.1V (Neta et al., 1988) presents a powerful oxidation capacity of antibiotics (Ahmed et al., 2012), e.g., destruction of antibiotics in pure water, underground water, domestic wastewater, and swine wastewater (Ahmed et al., 2012; Ahmed et al., 2014; Ben et al., 2009; Ji et al., 2014). However, little information is currently available with regard to the

remediation of antibiotics in pharmaceutical wastewater based on $\text{SO}_4^{\cdot-}$ oxidation.

Generally, generation efficiency of $\text{SO}_4^{\cdot-}$ controls the oxidation of antibiotics. Activated approaches of PMS or persulfate (PS) by such as photons (Ahmed et al., 2014; Kim H.Y. et al., 2015), heat (Ji et al., 2015; Qi et al., 2014), organic compound (Lei et al., 2015; Zhou et al., 2015), metal-based catalyst (Ayoub and Ghauch, 2014; Ghauch et al., 2013), transition metals (Ji et al., 2014) have been used to produce more $\text{SO}_4^{\cdot-}$ to eliminate organic contaminants. Among these activated methods, ferrous iron (Fe(II)) has the superiority of low cost, high activity, and environmental-friendly nature. Nonetheless, some intrinsic drawbacks of Fe(II)/PMS oxidation process have been gradually exposed. The slow conversion from Fe(III) back to Fe(II) is considered to be the major drawback of Fe(II)/PMS process (Zou et al., 2013). Chen et al. (2011) reported that hydroxylamine (NH_2OH , HA) could effectively accelerate the redox cycle of Fe(III) to Fe(II). Owing to the low rate constants with $\text{SO}_4^{\cdot-}$ (Neta et al., 1988) and HO^{\cdot} (Buxton et al., 1988), protonated HA can improve the degradation of benzoic acid (Zou et al., 2013), trichloroethylene (Tan et al., 2012), diuron (Wu et al., 2015), and Orange G (Han et al., 2014), as well as reducing the dosage of Fe(II) in Fe(II)/PMS or Fe(II)/PS system. To the best of our knowledge, few literature reported the enhancement of HA on the capacity of Fe(II)/PMS process applied in the pollution remediation of antibiotics.

Considering the bioactivity and potential risk arising from the toxicity of oxidation products of antibiotics, attention has to be paid to the degradation pathways of typical antibiotics in oxidation processes in order to assess the safety of treatment methods. Previous researches indicated the degradation products and pathways for same targets (e.g., SMX) were different in various $\text{SO}_4^{\cdot-}$ -based on oxidation processes (Ahmed et al., 2012; Ayoub and Ghauch, 2014; Gao et al., 2015; Ghauch et al., 2013; Ji et al., 2015). Qi et al (2014) reported the nitro derivative of SMX as an intermediate in microwave-activated persulfate process, but the same product were not found in ferrous-activated persulfate process (Ji et al., 2014). However, the lack of that information in the HA/Fe(II)/PMS process necessitates the study about degradation pathways and mechanism of antibiotics in the system.

Therefore, the objective of this study is to investigate the efficiency and mechanism of the HA/Fe(II)/PMS process in eliminating typical antibiotics. Sulfamethoxazole (SMX), one of the most widely used sulfonamide antibiotics to treat human and veterinary diseases as well as to promote the growth of food animals, was selected due to its frequent detection in the aquatic environment (Al Aukidy et al., 2012). The study is specifically focused on, (i) the degradation efficiency of SMX; (ii) the role of HA; (iii) the role of the reactive species involved; (iv) the identification of degradation products and possible transformation pathways in the HA/Fe(II)/PMS process, and (v) the treatment efficiency of SMX from the real pharmaceutical wastewater by the process.

2. Materials and methods

2.1. Materials

All chemicals were obtained from commercial sources and are listed in Text S1. All of these chemicals were used as received without further purification. Solutions were prepared in 18.2 M Ω cm Milli-Q water (Millipore). Stock solutions of ferrous sulfate and HA were prepared freshly with Milli-Q water everyday.

The raw pharmaceutical wastewater was collected from the effluent of secondary sedimentation tank of Fuhe pharmaceutical wastewater treatment plant located in Zhaodong, China. The raw wastewater was filtrated using 0.45 μm cellulose membrane and stored at 4 °C in dark before use.

2.2. Experimental procedure

All experiments were performed in 100 mL triangular flasks with a constant stirring rate with a PTFE-coated

magnetic stirrer at 25 ± 0.5 °C. The samples were covered with aluminum foil to avoid possible photodegradation. Each 30 mL reaction solution with desired concentrations of SMX or BA or SMX and BA, Fe(II), and HA, was prepared with ultrapure water or real pharmaceutical wastewater and adjusted to the initial desired pH with sodium hydroxide and sulfuric acid. Before the experiments were started, the reaction system was blown 15 min by high purity N₂ to eliminate the shadow of dissolved oxygen in solution. Each run was switched on by adding the desired dosage of PMS. Samples were withdrawn at set time intervals and quenched with excess pure methanol before analysis. The quenching experiments employed methanol and TBA as the quenchers, which were performed by adding desired alcohols into the reaction system and induced immediately after the addition of PMS. All experiments were repeated independently at least two times, and average values along with one standard deviation (\pm SD) were presented.

2.3. Analytical methods

The concentrations of SMX, BA, and *p*-HBA were determined by a high-performance liquid chromatography (HPLC, Waters e2695), and the detailed parameters are shown in [Text S2](#). Solution pH was measured by a pH meter (PHS-3C, Shanghai Rex). The concentration of ferric iron was measured at 300 nm ([Scharf, 1971](#)) with an UV-vis spectrometer (SP-752, Shanghai Spectrum), and the detailed procedure is shown in [Text S3](#). The degradation intermediates of SMX were detected by ultra-performance liquid chromatography coupled with electrospray ionization quadrupole time-of-flight mass spectrometry (UPLC-ESI-QTOFMS, Waters), the detailed parameters are shown in [Text S4](#). The analysis of water quality of real pharmaceutical wastewater is given in [Text S5](#).

3. Results and discussion

3.1. Degradation efficiency of SMX in HA/Fe(II)/PMS process

[Fig. 1](#) shows the degradation of SMX in HA/Fe(II)/PMS process. Less than 20% of SMX was degraded within 15 min in Fe(II)/PMS process, similar to that in PMS process. The low degradation efficiency could be due to the low Fe(II) concentration ([Anipsitakis and Dionysiou, 2004](#)). Surprisingly, HA (0.4 mM) improved the efficiency greatly and approximate 80% of SMX was degraded within 15 min in the HA/Fe(II)/PMS process. In comparison, HA in the PMS process inhibited the degradation of SMX degradation and only 10% of SMX was degraded within 15 min in HA/PMS process. It is possible that HA competed for and consumed PMS directly ([Han et al., 2014](#)). Therefore, HA and Fe(II) both should play a role in accelerating removal of SMX in the HA/Fe(II)/PMS process ([Wu et al., 2015](#)). The incomplete degradation of SMX in the HA/Fe(II)/PMS process might be due to the depletion of PMS ([Zou et al., 2013](#)). It should be pointed out that the HA/Fe(II)/PMS process exhibited an equivalent or even higher degradation efficiency of SMX, compared to reported catalytic PS oxidation processes ([Table S1](#)), e.g., Fe(II)/PS ([Ji et al., 2014](#)), thermo/PS ([Ji et al., 2015](#)), and Fe⁰/PS ([Ghauch et al., 2013](#)).

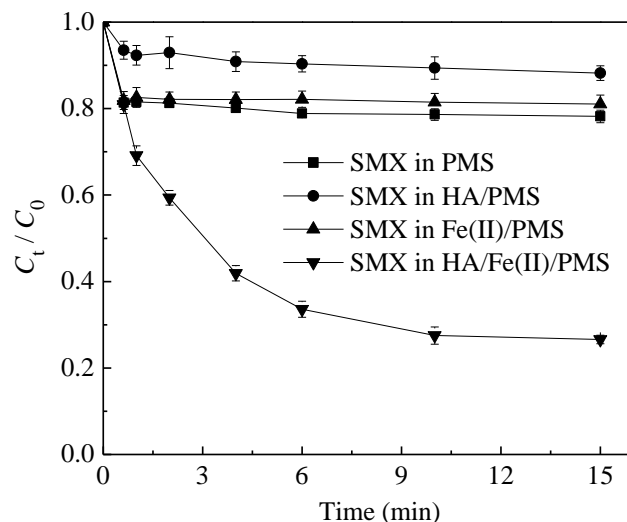


Fig. 1. Degradation of SMX in HA/Fe(II)/PMS process. Conditions: $[HA]_0 = 0.4$ mM (no addition in PMS and Fe(II)/PMS process), $[Fe(II)]_0 = 10$ μ M for HA/Fe(II)/PMS and Fe(II)/PMS process, $[PMS]_0 = 0.3$ mM, $[SMX]_0 = 20$ μ M, $pH_0 = 3.0$, 25 $^{\circ}$ C. Error bars represent the standard deviation from at least duplicate experiments.

3.2. Effect of pH on SMX degradation in HA/Fe(II)/PMS process

Solution pH determines the speciation distribution of HA, Fe(II), and Fe(III), and the self-decomposition kinetics of PMS. Fig. 2 shows the effect of initial pH on the degradation of SMX in the HA/Fe(II)/PMS process. No buffering agents were added to stabilize the solution pH in the experiments, and the variation of pH is given in the Fig. S1.

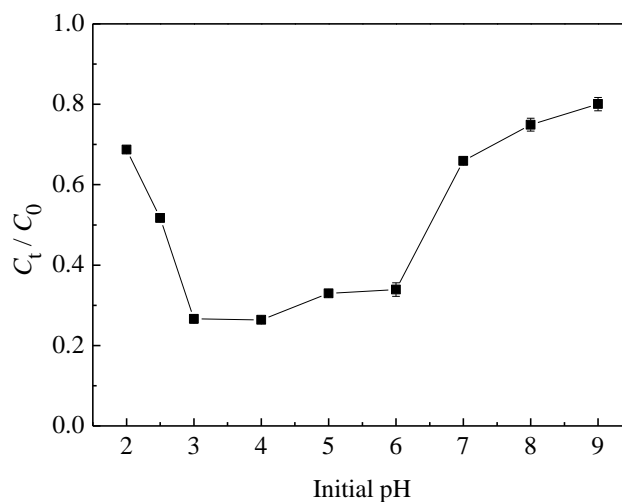


Fig. 2. Effect of initial pH on SMX degradation in HA/Fe(II)/PMS process. Conditions: $[HA]_0 = 0.40$ mM, $[Fe(II)]_0 = 10$ μ M, $[PMS]_0 = 0.3$ mM, $[SMX]_0 = 20$ μ M, $pH_0 = 2.0-9.0$, 25 $^{\circ}$ C and reaction time (T) = 15 min. Error bars represent the standard deviation from at least duplicate experiments.

From Fig. 2, the degradation of SMX was obviously promoted by increasing the initial pH from 2.0 to 3.0, reflecting the yield of reactive species could be improved greatly. The variation tendency could be mainly attributed to the formation and increase of $Fe(OH)_2$ with increasing solution pH. $Fe(OH)_2$ has been demonstrated to be more active than Fe(II) iron to activate peroxide and PMS (Wells and Salam, 1968; Zou et al., 2013). The optimal initial pH range is 3.0 to 6.0 in the system for degradation of SMX (the final balanced range of pH from 2.9

to 3.7 as shown in Fig. S1). And with further elevation of initial pH from 6.0 to 9.0 (the final balanced range of pH from 6.5 to 7.3 as shown in Fig. S1), the degradation of SMX was greatly inhibited. The decrease in SMX degradation efficiency in various degrees implies the inhibited generation of reactive species accordingly. Within the initial range of pH (3.0-9.0), on one hand, the yield of Fe(OH)₂ decreased by the increase of ferric oxyhydroxides precipitation above pH 3.0 (Flynn, 1984; Stefánsson, 2007), and the self-decomposition of PMS increased with the increase of solution pH (Ball and Edwards, 1956), which were bound to reduce the yield of reactive species directly. On the other hand, the primary form of HA is NH₂OH (pK_a = 5.96 and 13.74) (Hughes et al., 1971) at pH values in the range of 6.0 to 9.0. NH₂OH has high reaction rate constants with reactive radicals ($k_1 = 8.5 \times 10^8 \text{ M}^{-1} \text{ s}^{-1}$ for SO₄^{•-} (Neta et al., 1988), $k_2 = 9.5 \times 10^9 \text{ M}^{-1} \text{ s}^{-1}$ for HO[•] (Buxton et al., 1988)), which is comparable to that of SMX ($k_3 = 1.6 \times 10^{10} \text{ M}^{-1} \text{ s}^{-1}$ for SO₄^{•-}, $k_4 = 7.0 \times 10^9 \text{ M}^{-1} \text{ s}^{-1}$ for HO[•]) (Zhang et al., 2015). From the perspective of competition and consumption of radicals, NH₂OH would also decrease the contribution of reactive species to degrade SMX. Therefore, the speciation distribution of the involved species including HA, Fe(II), and Fe(III), and also the self-decomposition of PMS would be the dominant factors to influence the generation of reactive species and the degradation of SMX at different pH ranging from 2.0 to 9.0.

3.3. Role of HA in HA/Fe(II)/PMS Process

The aforementioned data and analysis suggest that HA plays an important role in improving the degradation efficiency of SMX in the HA/Fe(II)/PMS process. So, the effect of HA concentration on SMX degradation was investigated and the results are shown in Fig. 3. With the increase of HA concentration in the range of 0.0 to 0.4mM, the degradation efficiency of SMX obviously increased. Then increasing HA concentration continuously from 0.4 to 1.0mM, the improvement on the removal of SMX was found to be insignificant. Authors (Chen et al., 2011; Zou et al., 2013) reported that HA could effectively promote the redox cycle of Fe(III) to Fe(II), improve the generation of reactive species and increase the removal of organic pollutants at pH 3.0. However, excess HA could quench the reactive species (e.g., SO₄^{•-} and HO[•]) with a high reaction rate (Buxton et al., 1988; Neta et al., 1988) in HA/Fe(II)/PMS process at pH 3.0. Here, 0.4 mM of HA was optimum for SMX degradation and thus was used in the following experiment in this study.

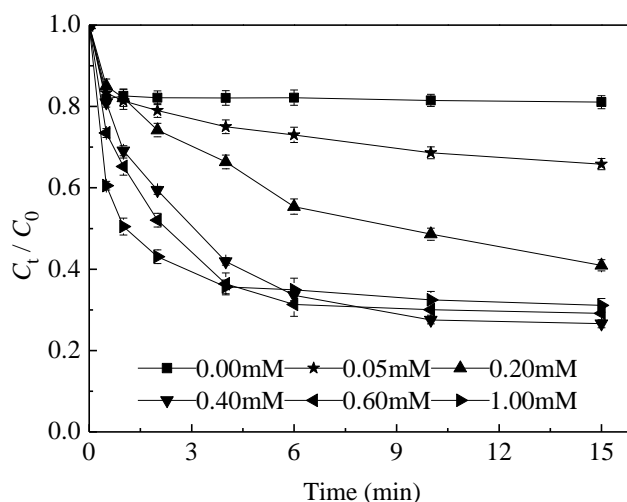


Fig. 3. Effect of HA concentration on SMX degradation in HA/Fe(II)/PMS Process. Conditions: [HA]₀ = 0.0-1.0 mM, [Fe(II)]₀ = 10 μM, [PMS]₀ = 0.3 mM, [SMX]₀ = 20 μM, pH₀ = 3.0, 25 °C. Error bars represent the standard deviation from at least duplicate

experiments.

For the sake of better understanding the role of HA, the variation of Fe(III) concentrations in Fe(II)/PMS process with/without SMX and HA/Fe(II)/PMS process with/without SMX were measured respectively. The results are shown in Fig. 4. The interference of HA and PMS on the measurement could be ignored at the experimental concentration (Chen et al., 2011; Zou et al., 2013). However, due to the obvious absorption of SMX and its degradation products at 300 nm, methanol was used to consume the reactive radicals (i.e., $\text{SO}_4^{\bullet-}$ and HO^{\bullet}) in the processes without SMX.

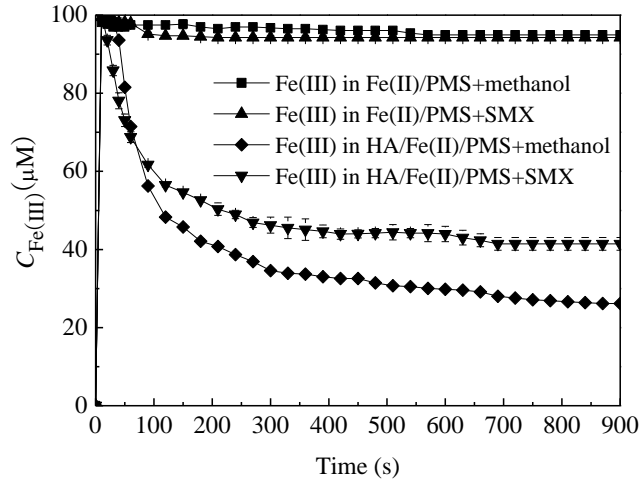
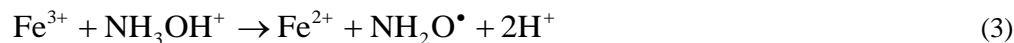


Figure 4. Effect of HA on Fe(III) concentration in HA/Fe(II)/PMS process. Conditions: $[\text{HA}]_0 = 0.40$ mM (no addition for Fe(II)/PMS process), $[\text{Fe(II)}]_0 = 100$ μM , $[\text{PMS}]_0 = 0.3$ mM, $[\text{SMX}]_0 = 20$ μM or $[\text{methanol}]_0 = 10$ mM, $\text{pH}_0 = 3.0$, 25 $^{\circ}\text{C}$. Error bars represent the standard deviation from at least duplicate experiments.

From Fig. 4, almost all Fe(II) was transformed into Fe(III) within 10 s and kept relatively steady throughout the runs in the Fe(II)/PMS processes without SMX and with SMX. This might be attributed to the fast reaction between Fe(II) and PMS via Eqs. (1) and (2) (Brandt and Van Eldik, 1995) and the slow transformation from Fe(III) to Fe(II). In the HA/Fe(II)/PMS processes without SMX and with SMX, the similar phenomenon about the generation of Fe(III) occurred within 10 s as the Fe(II)/PMS processes, however, the concentration of Fe(III) rapidly decreased after 10 s and then kept relatively steady after 300 s with the runs of reaction. It should be noted that the concentration of Fe(III) was reduced from approximate 100 μM to less than 42 μM and 27 μM in the HA/Fe(II)/PMS system with and without SMX, respectively. Moreover, the steady-state concentration of Fe(III) could be attributed to dynamic equilibrium of the iron ion circulation given in Eqs. (3)-(5) (Chen et al., 2011; Han et al., 2014). The higher steady-state concentration of Fe(III) in the system with SMX was probably due to the influence of target organics and intermediates on the UV absorption of solution at 300 nm. However, the decrease of Fe(III) concentration in both systems supports that the addition of HA intensively promoted the redox cycle of Fe(III) to Fe(II) and thus improved the removal of SMX in the HA/Fe(II)/PMS process.





3.4. Role of reactive radicals in HA/Fe(II)/PMS Process

It was reported that three reactive radicals (i.e., $\text{SO}_4^{\bullet-}$, HO^\bullet , and $\text{SO}_5^{\bullet-}$) could be generated during the catalyst-mediated decomposition of PMS (Brandt and Van Eldik, 1995; Maruthamuthu and Neta, 1977; Zou et al., 2013). Among these radicals, $\text{SO}_4^{\bullet-}$ and HO^\bullet are commonly known as the dominant reactive species for degrading aqueous organic contaminants in catalytic PMS oxidation processes (Gao et al., 2015; Ji et al., 2015; Zou et al., 2013). Based on the radical reaction characteristics, methanol and TBA were selected as quenching compounds to investigate their inhibition effects on SMX degradation, and thus explore the degradation mechanism of SMX in HA/Fe(II)/PMS process.

Fig. 5 shows the inhibitory effects of methanol and TBA on the degradation of SMX in the HA/Fe(II)/PMS process. From Fig. 5, it is obvious that HO^\bullet and $\text{SO}_4^{\bullet-}$ should be the responsible reactive species. The difference of inhibition effects between methanol and TBA were less than 10% in terms of SMX degradation, strongly suggesting a relatively weak contribution of $\text{SO}_4^{\bullet-}$ to the SMX degradation. Therefore, HO^\bullet could be the dominant reactive species for the degradation of SMX. The results agree with that obtained by Zou et al (2013) who had proved the major role of HO^\bullet in the degradation of BA in the same system. In addition, considering the relative inertia of alcohols toward $\text{SO}_5^{\bullet-}$ ($k \leq 10^3 \text{ M}^{-1} \text{ s}^{-1}$) (Hayon et al., 1972), approximately 25% of SMX degradation in non-alcohol system could be attributed to the rapid degradation in the initial reaction or the contribution of $\text{SO}_5^{\bullet-}$ which is similar to the degradation of BA in HA/Fe(II)/PMS process (Zou et al., 2013).

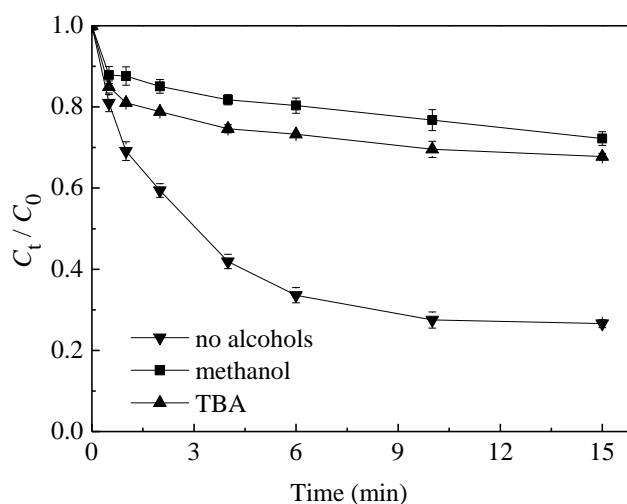


Fig. 5. Inhibition effect of radical scavengers on SMX degradation in HA/Fe(II)/PMS process. Conditions: $[\text{HA}]_0 = 0.40 \text{ mM}$, $[\text{Fe(II)}]_0 = 10 \text{ }\mu\text{M}$, $[\text{PMS}]_0 = 0.3 \text{ mM}$, $[\text{SMX}]_0 = 20 \text{ }\mu\text{M}$, $[\text{TBA}]_0 = 10 \text{ mM}$ or $[\text{methanol}]_0 = 10 \text{ mM}$, $\text{pH}_0 = 3.0$, $25 \text{ }^\circ\text{C}$. Error bars represent the

standard deviation from at least duplicate experiments.

In order to further confirm the major reactive species in the HA/Fe(II)/PMS process, the competition kinetics between SMX and BA were carried out and the results are shown in Fig. 6. Theoretically, the degradation of SMX and BA should agree with Eqs. (6) or (7) assuming that either HO[•] or SO₄^{•-} causes the degradation. The data of within 30 min (Fig. S2) was used considering the degradation trend of BA and SMX.

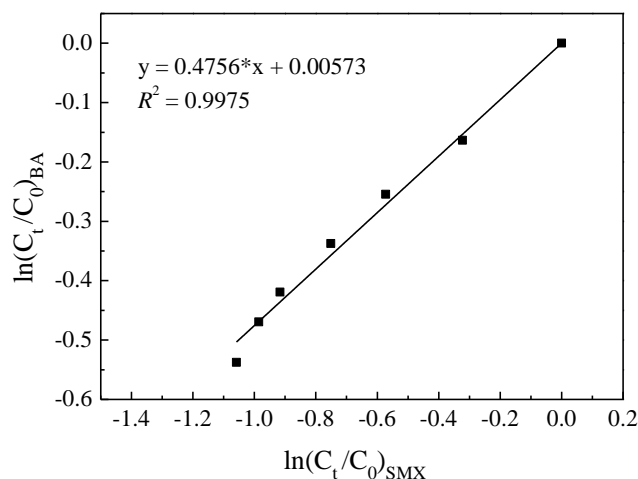


Fig. 6. Competition kinetics between SMX and BA with reactive species in HA/Fe(II)/PMS process. Conditions: [HA]₀ = 0.4 mM, [Fe(II)]₀ = 10 μM, [PMS]₀ = 0.3 mM, [SMX]₀ = 20 μM, [BA]₀ = 20 μM, pH = 3.0, 25 °C.

$$\frac{\ln\left(\frac{C_{t,BA}}{C_{0,BA}}\right)}{\ln\left(\frac{C_{t,SMX}}{C_{0,SMX}}\right)} = \frac{k_1}{k_2} \quad (6)$$

$$\frac{\ln\left(\frac{C_{t,BA}}{C_{0,BA}}\right)}{\ln\left(\frac{C_{t,SMX}}{C_{0,SMX}}\right)} = \frac{k_1'}{k_2'} \quad (7)$$

Here, k_1 and k_2 are the rate constants of HO[•] with BA and SMX, respectively; k_1' and k_2' are the rate constants of SO₄^{•-} with BA and SMX, respectively. At pH 3.0, $k_1 = 4.3 \times 10^9 \text{ M}^{-1} \text{ s}^{-1}$ (Buxton et al., 1988), $k_2 = 7.0 \times 10^9 \text{ M}^{-1} \text{ s}^{-1}$ (Zhang et al., 2015), $k_1' = 1.2 \times 10^9 \text{ M}^{-1} \text{ s}^{-1}$ (Neta et al., 1988), and $k_2' = 1.6 \times 10^{10} \text{ M}^{-1} \text{ s}^{-1}$ (Zhang et al., 2015). Thus, $k_1 / k_2 = 0.614$, and $k_1' / k_2' = 0.075$.

The slope in Fig. 6 for the competition kinetics is about 0.4756, approaching k_1 / k_2 , but deviating far from k_1' / k_2' . This agreement indeed validated the dominant role of HO[•] in the system. Furthermore, the formation of p-HBA (Fig. S3) also confirmed the contribution of HO[•] to the degradation of BA and SMX (Klein et al., 1975). It was noted that the formation ratio of p-HBA didn't agree with the reported one of about 1/5.87 (Zhou and Mopper, 1990), possibly ascribed to the attack of HBA or their intermediate precursors by Fe(III) and persulfate (Duesterberg and Waite, 2007).

3.5. Degradation products and pathways of SMX in HA/Fe(II)/PMS process

To further study the degradation mechanism of SMX in HA/Fe(II)/PMS process, UPLC-ESI-QTOFMS was

employed to identify the transformation intermediates. The HPLC chromatogram of major degradation intermediates are shown in Fig. S4. A total of eight oxidation products, P-93, P-98, P-155, P-189, P-267, P-269, P-270, P-283, were identified in the HA/Fe(II)/PMS process. The corresponding product ion spectrum and the proposed fragment structures are shown in Fig. S5. Among these products, only P-98 and P-270 had been detected in Fe(II)/PS process (Ji et al., 2014).

Based on the accurate mass spectrum of degradation product in Fig. S6, P-98 ($m/z = 99$ for MH^+) was identified as 3-amino-5-methylisoxazole, which was attributed to the cleavage of S-N bond in SMX. P-98 had also been detected in other oxidation processes based on sulfate radical oxidation (Ahmed et al., 2012; Ghauch et al., 2013; Ji et al., 2014; Ji et al., 2015). Accompanying with the yield of P-98, another intermediate, P-155, would also be yielded and be transformed to P-189 ($m/z = 190$ for MH^+) partially. Combining the daughter ion spectrums of P-155 and P-189 (Fig. S7 and S8), P-155 and P-189 were identified as 4-sulfonylcyclohexa-2,5-dien-1-imine and hydroxysulfanilic acid, respectively. P-189, as a well-known product, had been identified in various catalytic PS processes (Gao et al., 2015; Qi et al., 2014), nevertheless, P-155 was only found in ozonation process (Gómez-Ramos et al., 2011). In addition, P-155 and P-189 could be further transformed as aniline (P-93, $m/z = 94$ for MH^+) to some degree as shown in Fig. S5 (Gao et al., 2015; Ji et al., 2015).

The fragment at $m/z = 284$ for MH^+ (i.e., P-283) in Fig. S5 was another primary intermediate. Several primary ion fragments ($m/z = 98, 122, 138, 178, 193, 203$ and 220) occurred in the daughter ion spectrum of P-283 (Fig. S9). Studies have reported the ion fragments at $m/z = 122$ and $m/z = 138$ were identified as nitro benzene ($C_6H_4NO_2$) (Gao et al., 2014) and nitro phenol (Abellán et al., 2008), respectively. Thus, the structure of P-283 was proposed as nitro SMX (Ahmed et al., 2012; Ji et al., 2015). The proposed fragmentation pathways and structures of daughter ions of P-283 are shown in Fig. S9. In addition, P-267 ($m/z = 268$ for MH^+) and P-269 ($m/z = 270$ for MH^+) were both detected during the degradation of SMX in the HA/Fe(II)/PMS process. The accurate mass spectrum of P-267 with daughter ion fragments at $m/z = 107, 160, 146, 188, 204$ (Fig. S10) shows P-267 was the nitroso derivative of SMX (Ahmed et al., 2012), which was ultimately oxidized as nitro group ($-NO_2$) and conformed P-283. The identification of P-267 and P-283 suggested the amino group ($-NH_2$) on the aromatic ring of SMX was susceptible to be attack by reactive radicals. Therefore, the hydroxylamine derivative of SMX (P-269 with $m/z = 270$ for MH^+) could be yielded before the conformation of P-267 and P-283. P-269, as an intermediate, was also found during the oxidation of SMX in heat/PS process (Gao et al., 2015).

For P-270 ($m/z = 271$ for MH^+), two primary ion fragments ($m/z = 99$ and 175 for MH^+) occurred in the daughter ion spectrum of 271 (Fig. S11), which indicated the formation of a hydroxylated derivative of SMX. Furthermore, the loss of methyl group to yield the fragment with $m/z = 256$ and the losses of methyl group and oxygen to yield the fragment with $m/z = 230$ also confirmed the addition of hydroxyl group to the benzene ring of SMX. The proposed structures of fragments and position of hydroxyl group is shown in Fig. S11. P-270 had also been reported as an intermediate of the degradation of SMX in the processes of Fe(II)/PS (Ji et al., 2014), Cobalt(II)/PMS (Ahmed et al., 2012), thermo/PS (Ji et al., 2015), and microwave/PS (Qi et al., 2014).

Combined with the identification of oxidation intermediates, three major transformation pathways (A, B, and C) are proposed in Fig. 7, where the reactive species (HO^\bullet and $SO_4^{\bullet-}$) could attack the reaction sites of S-N bond, amine group on the aromatic ring, and benzene ring in SMX, respectively. On the basis of aforementioned discussion, HO^\bullet was validated to be the predominant reactive species for the degradation of SMX in the HA/Fe(II)/PMS process. Therefore, HO^\bullet definitely played a key role for the proposed pathways of SMX. In general, HO^\bullet likely reacts with organic compounds by radical adduct formation, hydrogen atom abstraction, and single electron transfer (An et al., 2014). For pathway A, after the S-N bond in the SMX was attacked by HO^\bullet ,

3-amino-5-methylisoxazole (P-98) and 4-sulfonylcyclohexa-2,5-dien-1-imine (P-155) were formed. Subsequently, the addition of HO[•] to the reaction sites of –SO₂ and –NH in P-155 resulted in the formation of hydroxysulfanilic acid (P-189). P-189 could be further oxidized to lose sulfuric acid and finally yield aniline (P-94), which indicated the reactivity of sulfonated moiety with HO[•] (Gonçalves et al., 2012). For the pathway B, hydroxylamine derivative of SMX (P-269) with *m/z* of [M+16]⁺ indicated the attack of HO[•] through abstracting the hydrogen of –NH₂ to form hydroxylamine moiety (Dirany et al., 2012). The hydroxylamine moiety of P-269 could be further oxidized by HO[•] to yield nitroso-SMX (P-267) and nitro-SMX (P-283) (Kim C. et al., 2015). Meanwhile, the S-N bond of P-269 was also probably cleaved through hydrogen abstraction and addition of HO[•] to transform as P-98 and P-189 (Ji et al., 2015). In addition, the direct addition of HO[•] to benzene ring of SMX could form hydroxylated SMX (P-270) through pathway C (Hu et al., 2007).

However, considering the existence of SO₄^{•-} in HA/Fe(II)/PMS system, to some extent, the degradation products of SMX could also be generated by attack of SO₄^{•-} on the above sites of SMX through electron-transfer mechanism (Neta et al., 1977). Especially, as a preferred reactive site of SO₄^{•-}, the amino and imino moiety was easily to be oxidized by SO₄^{•-} and transformed as P-189 (Qi et al., 2014) and P-269 (Gao et al., 2015). Ji et al (2015) and Yan et al (2011) also noted that SO₄^{•-} was responsible for the formation of hydroxylated SMX.

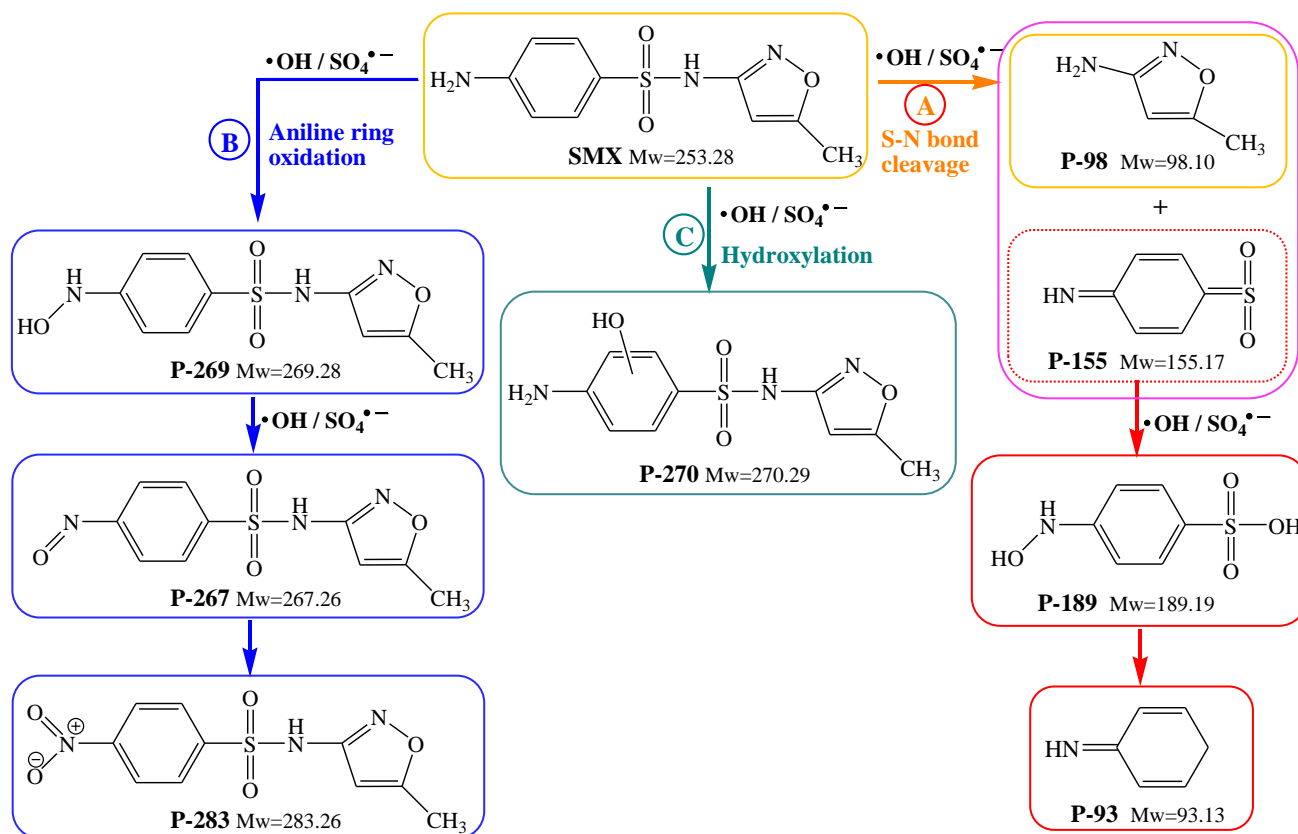


Fig. 7. Proposed transformation pathways for SMX degradation in HA/Fe(II)/PMS process.

3.6. Degradation of SMX in real pharmaceutical wastewater

To examine the efficiency of HA/Fe(II)/PMS process in realistic wastewater, experiments were performed in the real pharmaceutical wastewater (the water quality is shown in Table S2). Fig. 8 shows the degradation of SMX by HA/Fe(II)/PMS process in the wastewater sample. The process exhibited good capacity to remove SMX and total organic carbon (TOC) from the wastewater sample. Approximately 70% of SMX and 50% of TOC (Fig. S12) were

removed within 15 min at PMS dosage of 2.0 mM and Fe(II) dosage of 20.6 μM , respectively. The efficiency was comparable to that of Cobalt(II)/PMS reported by Ahmed et al (2012) (Table S1). Although the removal rates of SMX were reduced with the decreased dosage of PMS, the degradation of SMX were almost finished within the first 4 min. The similar phenomenon was also reported in a previous study about the degradation of SMX in swine wastewater by Fenton process (Ben et al., 2009), and it was probably due to the fast generation of and attack from the reactive species (e.g., HO^\bullet and $\text{SO}_4^{\bullet-}$) in the initial period of reaction.

Furthermore, compared with the Milli-Q water sample (Fig. S13), the coexisting water components in the wastewater sample only inhibited approximately 7% of SMX degradation within 15min at PMS dosage of 0.3 mM and Fe(II) dosage of 20.6 μM . Although a high concentration of chloride (6.7 mM) was detected in the pharmaceutical wastewater, the degradation of SMX was hardly influenced by the chloride (Fig. S13) as reported by Zhang et al. (2015). Therefore, the other coexisting components (especially organic contaminants) in the real wastewater could be the dominant factor to result in the reduction of SMX removal rate. However, the comparison of SMX degradation in different water samples indicated that the HA/Fe(II)/PMS process exhibited a strong selective oxidation of SMX in the wastewater sample.

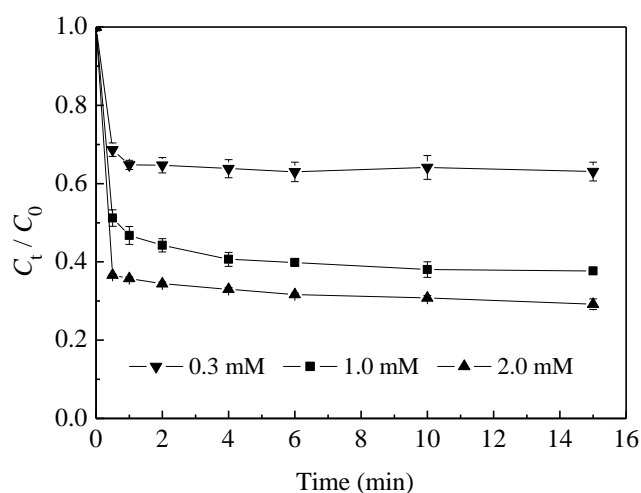


Fig. 8. Effect of PMS concentration on the degradation of SMX in real pharmaceutical wastewater in HA/Fe(II)/PMS process. Conditions: $[\text{HA}]_0 = 0.4 \text{ mM}$, $[\text{Fe(II)}]_0 = 20.6 \mu\text{M}$, $[\text{PMS}]_0 = 0.3\text{--}2.0 \text{ mM}$, $[\text{SMX}]_0 = 31.3 \mu\text{M}$, $\text{pH} = 5.0$, $25 \text{ }^\circ\text{C}$. Error bars represent the standard deviation from at least duplicate experiments.

4. Engineering Implications

In HA/Fe(II)/PMS process, the transformation of Fe(III) to Fe(II) was strongly promoted with the addition of HA, so that a low Fe(II) concentration at several micromolar (μM) was enough to remove approximately 70% of SMX (Fig. 8) and 50% of TOC (Fig. S12) from realistic wastewater at pH 5.0. Such a low concentration of Fe(II) could efficiently alleviate the accumulation of ferric oxide sludge in conventional Fe(II)/PMS process. Although hydroxylamine is a toxic compound, it can be decomposed completely by catalysts such as transition metals with enough dosage of oxygen or air at ambient temperature with environmentally benign by-products (nitrogen and water) (Gomez et al., 1990; Song et al., 2008). Considering the efficient generation of powerful oxidants like HO^\bullet and the more selective oxidant like $\text{SO}_4^{\bullet-}$, the HA/Fe(II)/PMS process might be a promising process to remove SMX even other antibiotics and refractory organic contaminants from wastewater.

5. Conclusions

In this research, the HA/Fe(II)/PMS process was adopted to degrade SMX and exhibited an effective degradation capacity. The enhanced degradation efficiency in a wider range of solution pH (3.0-6.0) in the HA/Fe(II)/PMS process was attributed to the enhancement of HA through accelerating the conversion from Fe(III) back to Fe(II). The optimum dosage of HA depended on the concentration of PMS and pH, and the excess HA inhibited the degradation by reacting with PMS and quenching the reactive species. The degradation of SMX was initiated by $\text{SO}_4^{\cdot-}$ and HO^{\cdot} , although HO^{\cdot} played the dominant role. Eight intermediates of SMX were produced via the cleavage of S-N bond, oxidation of amine group on the aromatic ring and hydroxylation of the benzene ring in the system. The process also exhibited an effective removal of SMX and coexisting other organic pollutants (i.e., TOC) in the real pharmaceutical wastewater.

Acknowledgement

This work was supported by the National Natural Science Foundation of China (21307057), the China Scholarship Council (201406685037), the Postdoctoral Science Foundation of Heilongjiang Province (LBH-Z13062), the Natural Science Foundation of Jiangsu Province (BK20130577), the Specialized Research Fund for the Doctoral Program of Higher Education of China (SRFDP, 20130091120014), and the Fundamental Research Funds for the Central Universities (20620140128). The authors sincerely thank Associate Professor Jimin Shen, Jing Zou (Harbin Institute of Technology) for their technical help with the UPLC-ESI-QTOFMS, HPLC, ion chromatography analysis.

Reference

- Abellán, M.N., Gebhardt, W., Schröder, H.Fr., 2008. Detection and identification of degradation products of sulfamethoxazole by means of LC/MS and $-\text{MS}^n$ after ozone treatment. *Water Sci. Technol.* 58 (9), 1803-1812.
- Ahmed, M.M., Brienza, M., Goetz, V. Chiron, S., 2014. Solar photo-Fenton using peroxymonosulfate for organic micropollutants removal from domestic wastewater: Comparison with heterogeneous TiO_2 photocatalysis. *Chemosphere.* 117, 256-261.
- Ahmed, M.M., Barbati, S., Doumenq, P., Chiron, S., 2012. Sulfate radical anion oxidation of diclofenac and sulfamethoxazole for water decontamination. *Chem. Eng. J.* 197, 440-447.
- Al Aukidy, M., Verlicchi, P., Jelic, A., Petrovic, M., Barcelò, D., 2012. Monitoring release of pharmaceutical compounds: Occurrence and environmental risk assessment of two WWTP effluents and their receiving bodies in the Po Valley, Italy. *Sci. Total Environ.* 438, 15-25.
- An, T., Gao, Y., Li, G., Kamat, P.V., Peller, J., Joyce, M.V., 2014. Kinetics and mechanism of $(\bullet)\text{OH}$ mediated degradation of dimethyl phthalate in aqueous solution: experimental and theoretical studies. *Environ. Sci. Technol.* 48 (1), 641-648.
- Anipsitakis, G.P., Dionysiou, D.D., 2004. Radical generation by the interaction of transition metals with common oxidants. *Environ. Sci. Technol.* 38 (13), 3705-3712.
- Ayoub, G., Ghauch, A., 2014. Assessment of bimetallic and trimetallic iron-based systems for persulfate activation: Application to sulfamethoxazole degradation. *Chem. Eng. J.* 256, 280-292.
- Ball, D.L., Edwards, J.O., 1956. The kinetics and mechanism of the decomposition of Caro's acid. *J. Am. Chem. Soc.* 78 (6), 1125-1129.
- Ben, W., Qiang, Z., Pan, X., Chen, M., 2009. Removal of veterinary antibiotics from sequencing batch reactor (SBR) pretreated swine wastewater by Fenton's reagent. *Water Res.* 43 (17), 4392-4402.

- Brandt, C., Van Eldik, R., 1995. Transition Metal-Catalyzed Oxidation of Sulfur(IV) Oxides. Atmospheric-Relevant Processes and Mechanisms. *Chem. Rev.* 95 (1), 119-190.
- Buxton, G.V., Greenstock, C.L., Helman, W.P., Ross, A.B., 1988. Critical-review of rate constants for reactions of hydrated electrons, hydrogen-atoms and hydroxyl radicals ($\bullet\text{OH}/\bullet\text{O}$) in aqueous solution. *J. Phys. Chem. Ref. Data.* 17 (2), 513-886.
- Chen, L., Ma, J., Li, X., Zhang, J., Fang, J., Guan, Y., Xie, P., 2011. Strong Enhancement on fenton oxidation by addition of hydroxylamine to accelerate the ferric and ferrous iron cycles. *Environ. Sci. Technol.* 45 (9), 3925-3930.
- De Amorim, K.P., Romualdo, L.L., Andrade, L.S., 2013. Electrochemical degradation of sulfamethoxazole and trimethoprim at boron-doped diamond electrode: Performance, kinetics and reaction pathway. *Sep. Purif. Technol.* 120, 319-327.
- Dirany, A., Sirés, I., Oturan, N., Özcan, A., Oturan, M.A., 2012. Electrochemical treatment of the antibiotic sulfachloropyridazine: Kinetics, reaction pathways, and toxicity evolution. *Environ. Sci. Technol.* 46 (7), 4074-4082.
- Duesterberg, C.K., Waite T.D., 2007. Kinetic modeling of the oxidation of p-Hydroxybenzoic acid by Fenton's reagent: Implications of the role of quinones in the redox cycling of iron. *Environ. Sci. Technol.* 41 (11), 4103-4110.
- Flynn, C.M., 1984. Hydrolysis of inorganic iron (III) salts. *Chem. Rev.* 84 (1), 31-41.
- Gao, S., Zhao, Z., Xu, Y., Tian, J., Qi, H., Lin, W., Cui, F., 2014. Oxidation of sulfamethoxazole (SMX) by chlorine, ozone and permanganate - A comparative study. *J. Hazard. Mater.* 274, 258-269.
- Gao, Y., Gao, N., Deng, Y., Yin, D., Zhang, Y., Rong, W., Zhou, S., 2015. Heat-activated persulfate oxidation of sulfamethoxazole in water. *Desalin. Water Treat.* 56 (8), 2225-2233.
- Ghauch, A., Ayoub, G., Naim, S., 2013. Degradation of sulfamethoxazole by persulfate assisted micrometric Fe^0 in aqueous solution. *Chem. Eng. J.* 228, 1168-1181.
- Gomez, E., Estela, J.M., Cerda, V., 1990. Thermometric determination of Cu^{II} based on its catalytic effect on the oxidation of hydroxylamine by dissolved oxygen. *Thermochim. Acta.* 165 (2), 255-260.
- Gómez-Ramos, M.M., Mezcua, M., Agüera, A., Fernández-Alba, A.R., Gonzalo, S., Rodríguez, A., Rosal, R., 2011. Chemical and toxicological evolution of the antibiotic sulfamethoxazole under ozone treatment in water solution. *J. Hazard. Mater.* 192 (1), 18-25.
- Gonçalves, A.G., Órfão, J.J.M., Pereira, M.F.R., 2012. Catalytic ozonation of sulphamethoxazole in the presence of carbon materials: Catalytic performance and reaction pathways. *J. Hazard. Mater.* 239-240, 167-174.
- Han, D., Wan, J., Ma, Y., Wang, Y., Huang, M., Chen, Y., Li, D., Guan, Z., Li, Y., 2014. Enhanced decolorization of Orange G in a $\text{Fe}(\text{II})$ -EDDS activated persulfate process by accelerating the regeneration of ferrous iron with hydroxylamine. *Chem. Eng. J.* 256, 316-323.
- Hayon, E., Treinin, A., Wilf, J., 1972. Electronic spectra, photochemistry, and autoxidation mechanism of the sulfite-bisulfite-pyrosulfite systems. SO_2^- , SO_3^- , SO_4^- , and SO_5^- radicals. *J. Am. Chem. Soc.* 94 (1), 47-57.
- Hu, L., Flanders, P.M., Miller, P.L., Strathmann, T.J., 2007. Oxidation of sulfamethoxazole and related antimicrobial agents by TiO_2 photocatalysis. *Water Res.* 41 (12), 2612-2626.
- Hughes, M.N., Nicklin, H.G., Shrimanker, K., 1971. Autoxidation of hydroxylamine in alkaline solutions. Part II. Kinetics. The acid dissociation constant of hydroxylamine. *J. Chem. Soc. A.* 3485-3487.
- Ji, Y., Fan, Y., Liu, K., Kong, D., Lu, J., 2015. Thermo activated persulfate oxidation of antibiotic sulfamethoxazole and structurally related compounds. *Water Res.* 87, 1-9.

- Ji, Y., Ferronato, C., Salvador, A., Yang, X., Chovelon, J., 2014. Degradation of ciprofloxacin and sulfamethoxazole by ferrous-activated persulfate: Implications for remediation of groundwater contaminated by antibiotics. *Sci. Total Environ.* 472, 800-808.
- Kim, C., Panditi, V.R., Gardinali, P.R., Varma, R.S., Kim, H., Sharma, V.K., 2015. Ferrate promoted oxidative cleavage of sulfonamides: Kinetics and product formation under acidic conditions. *Chem. Eng. J.* 279, 307-316.
- Kim, H.Y., Kim, T., Yu, S., 2015. Photolytic degradation of sulfamethoxazole and trimethoprim using UV-A, UV-C and vacuum-UV (VUV). *J. Environ. Sci. Health. A.* 50 (3), 292-300.
- Klein, G.W., Bhatia, K., Madhavan, V., Schuler, R.H., 1975. Reaction of $\bullet\text{OH}$ with benzoic acid. Isomer distribution in the radical intermediates. *J. Phys. Chem.* 79 (17), 1767-1774.
- Kümmerer, K., 2009. Antibiotics in the aquatic environment - A review - Part I. *Chemosphere.* 75 (4), 417-434.
- Larsson, D.G.J., de Pedro, C., Paxeus, N., 2007. Effluents from drug manufactures contains extremely high levels of pharmaceuticals. *J. Hazard. Mater.* 148 (3), 751-755.
- Lei, Y., Zhang, H., Wang, J., Ai, J., 2015. Rapid and continuous oxidation of organic contaminants with ascorbic acid and a modified ferric/persulfate system. *Chem. Eng. J.* 270, 73-79.
- Maruthamuthu, P., Neta, P., 1977. Radiolytic chain decomposition of peroxomonophosphoric and peroxomonosulfuric acids. *J. Phys. Chem.* 81 (10), 937-940.
- Marx, C., Mühlbauer, V., Krebs, P., Kuehn, V., 2015. Environmental risk assessment of antibiotics including synergistic and antagonistic combination effects. *Sci. Total Environ.* 524-525, 269-279.
- Michael, I., Rizzo, L., McArdell, C.S., Manaia, C.M., Merlin, C., Schwartz, T., Dagot, C., Fatta-Kassinos, D., 2013. Urban wastewater treatment plants as hotspots for the release of antibiotics in the environment: A review. *Water Res.* 47 (3), 957-995.
- Neta, P., Huie, R.E., Ross, A.B., 1988. Rate constants for reactions of inorganic radicals in aqueous solution. *J. Phys. Chem. Ref. Data.* 17 (3), 1027-1284.
- Neta, P., Madhavan, V., Zemel, H., Fessenden, R.W., 1977. Rate constants and mechanism of reaction of sulfate radical anion with aromatic compounds. *J. Am. Chem. Soc.* 99 (1), 163-164.
- Pomati, F., Castiglioni, S., Zuccato, E., Fanelli, R., Vigetti, D., Rossetti, C., Calamari, D., 2006. Effects of a complex mixture of therapeutic drugs at environmental levels on human embryonic cells. *Environ. Sci. Technol.* 40 (7), 2442-2447.
- Qi, C., Liu, X., Lin, C., Zhang, X., Ma, J., Tan, H., Ye, W., 2014. Degradation of sulfamethoxazole by microwave-activated persulfate: Kinetics, mechanism and acute toxicity. *Chem. Eng. J.* 249, 6-14.
- Rivera-Utrilla, J., Sánchez-Polo, M., Ferro-García, M.Á., Prados-Joya, G., Ocampo-Pérez, R., 2013. Pharmaceuticals as emerging contaminants and their removal from water. A review. *Chemosphere.* 93 (7), 1268-1287.
- Ryan, C.C., Tan, D.T., Arnold, W.A., 2011. Direct and indirect photolysis of sulfamethoxazole and trimethoprim in wastewater treatment plant effluent. *Water Res.* 45 (3), 1280-1286.
- Scharf, K., 1971. Spectrophotometric measurement of ferric ion concentration in the ferrous sulphate (Fricke) dosimeter. *Phys. Med. Biol.* 16 (1), 77-86.
- Song, W., Li, J., Liu, J., Shen, W., 2008. Production of hydrogen peroxide by the reaction of hydroxylamine and molecular oxygen over activated carbons. *Catal Commun.* 9 (5), 831-836.
- Stefánsson, A., 2007. Iron (III) hydrolysis and solubility at 25 °C. *Environ. Sci. Technol.* 41 (17), 6117-6123.
- Tan, C., Gao, N., Chu, W., Li, C., Templeton, M.R., 2012. Degradation of diuron by persulfate activated with

ferrous ion. *Sep. Purif. Technol.* 95, 44-48.

- Wells, C.F., Salam, M.A., 1968. The effect of pH on the kinetics of the reaction of iron (II) with hydrogen peroxide in perchlorate media. *J. Chem. Soc. A.* 24-29.
- Wu, X., Gu, X., Lu, S., Qiu, Z., Sui, Q., Zang, X., Miao, Z., Xu, M., 2015. Strong enhancement of trichloroethylene degradation in ferrous ion activated persulfate system by promoting ferric and ferrous ion cycles with hydroxylamine. *Sep. Purif. Technol.* 147, 186-193.
- Yan, J., Lei, M., Zhu, L., Anjum, M.N., Zou, J., Tang, H., 2011. Degradation of sulfamonomethoxine with Fe₃O₄ magnetic nanoparticles as heterogeneous activator of persulfate. *J. Hazard. Mater.* 186 (2-3), 1398-1404.
- Zhang, R., Sun, P., Boyer, T.H., Zhao, L., Huang, C., 2015. Degradation of pharmaceuticals and metabolite in synthetic human urine by UV, UV/H₂O₂, and UV/PDS. *Environ. Sci. Technol.* 49 (5), 3056-3066.
- Zhou, X., Mopper, K., 1990. Determination of photochemically produced hydroxyl radicals in seawater and freshwater. *Mar. Chem.* 30, 71-88.
- Zhou, Y., Jiang, J., Gao, Y., Ma, J., Pang, S., Li, J., Lu, X., Yuan, L., 2015. Activation of peroxymonosulfate by benzoquinone: A novel nonradical oxidation process. *Environ. Sci. Technol.* 49 (21), 12941-12950.
- Zou, J., Ma, J., Chen, L., Li, X., Guan, Y., Xie, P., Pan, C., 2013. Rapid acceleration of ferrous iron/peroxymonosulfate oxidation of organic pollutants by promoting Fe(III)/Fe(II) cycle with hydroxylamine. *Environ. Sci. Technol.* 47 (20), 11685-11691.